Nonlocal (Pair Site) Reactivity from Second-Order Static Density Response Function: Gas- and Solution-Phase Reactivity of the Acetaldehyde Enolate as a Test Case

Renato Contreras,*,†,‡ Luis R. Domingo,*,§ Juan Andrés,† Patricia Pérez,†,‡ and Orlando Tapia‡

Departament de Ciènces Experimentals, Universitat Jaume I, Box 242, 12080, Castelló, Spain, Departament de Química Orgànica, Universitat de València, Dr. Moliner 50, 46100 Burjassot, València, Spain, and Department of Physical Chemistry, Uppsala University, Box 532, S-751 21, Uppsala, Sweden

Received: June 29, 1998; In Final Form: November 4, 1998

A nonlocal (pair site) reactivity scheme is developed and tested. The theory is cast in terms of the first-order Fukui response function $f(\mathbf{r},\mathbf{r}')$, previously proposed by Fuentealba and Parr [*J. Chem. Phys.* **1991**, *94*, 5559]. A change of variables is introduced by using the softness $s(\mathbf{r})$ and $t(\mathbf{r}) = [\partial s(\mathbf{r})/\partial N]_{v(\mathbf{r})}$ (the variation of softness with respect to the changes in the total number of electrons N at constant external potential $v(\mathbf{r})$) that leads to a simple expression for the variation of the Fukui function at site k, namely $\Delta f_k^- = A_k^- \delta\nu_k - t_k^- \Delta\mu$ for an electrophilic attack. The first term describes a local contribution, proportional to the variation of the electrostatic potential that can be induced, for example, by the approach of an electrophilic agent, with a variable global softness coefficient thereby incorporating higher (third) order derivatives of the electronic energy. The second term contains nonlocal information implicitly involving a second reactive site that is expressed in terms of the variations to the electronic chemical potential $\Delta\mu$, accounting for the charge transfer related to the electrophile/nucleophile interaction. New reactivity indexes t_k^+, t_k^-, t_k^* are derived. They are associated with nucleophile, electrophile, and radical attacks. The theory applies to gas-phase reactivity. Solvent effects are introduced in the continuum approach to the surrounding medium. The resulting model is applied to study the chemistry of the enolate ion in the gas and solution phases. In the gas phase, an inversion of $f(\mathbf{r})$ in the vicinity of the transition structure is observed that leads to alkylation at the oxygen atom. Incorporation of two water molecules to mimic solvent effects changes the gas-phase pattern of reactivity, and alkylation at the α-carbon is predicted in solution, in agreement with the experiments.

1. Introduction

Predicting changes in reactivity and selectivity at particular atom centers of a given molecule produced by reactants or any other external source of perturbation, such as solvent effects, has always been an important problem in chemistry, biochemistry, pharmacology, and molecular biology.[1] This has been a goal of quantum chemical reactivity indexes that were created and developed since the dawn of theoretical chemistry. The successes of the density functional theory in calculating the electronic structure of molecules have prompted the extension of local reactivity indexes to study molecular reactivity. In a previous work[2] (hereafter referred to as part 1), we have presented a model to deal with nonlocal (pair site) reactivity based on two approaches to the first-order static-density response function $\chi(\mathbf{r},\mathbf{r}')$, for a constant number of electrons N. The first one, derived by Berkowitz and Parr,[3] is a suitable formulation for its applications in chemistry, as it is expressed in terms of nonlocal, local, and global electronic descriptors of chemical reactivity, namely

$$\chi(\mathbf{r},\mathbf{r}') = \left[\frac{\delta\rho(\mathbf{r})}{\delta\nu(\mathbf{r}')}\right]_N = -s(\mathbf{r},\mathbf{r}') + \frac{s(\mathbf{r})s(\mathbf{r}')}{S} \qquad (1)$$

This response function may be used to describe changes in the electronic density $\rho(\mathbf{r})$ when the system is locally perturbed at a different point $\mathbf{r}'$, by an additional external source that adds to the external potential $v°(\mathbf{r}')$.[3] This quantity is expressed in terms of the nonlocal softness kernel $s(\mathbf{r},\mathbf{r}')$ and the local and global softness $s(\mathbf{r})$ and S, respectively. As a result of the complexity of the definition of the softness kernel, this quantity may be treated on an approximated basis only, yielding useful applications of eq 1 to different chemical problems.[4,5] The simplest approach to $s(\mathbf{r},\mathbf{r}')$, is the local approximation proposed by Vela and Gázquez,[5] namely, $s(\mathbf{r},\mathbf{r}') = f(\mathbf{r})S\delta(\mathbf{r} - \mathbf{r}')$, where $\delta(\mathbf{r} - \mathbf{r}')$ is the Dirac distribution.

The function $f(\mathbf{r})$ is the Fukui function. It corresponds to the first derivative of $\rho(\mathbf{r})$, with respect to the total number of electrons N, at constant external potential. Use of this local approximation yields a simple expression for the changes in electron density at any point $\mathbf{r}$ in space, which after some approximations lead to the working formula[2]

$$\mathrm{d}\rho(\mathbf{r}) = -s°(\mathbf{r})\,\mathrm{d}u(\mathbf{r}) \qquad (2)$$

in terms of the modified potential variations $\delta u(\mathbf{r}) = \delta v(\mathbf{r}) - \Delta\mu$. Equation 2, up to first order of the electron density at a molecular region, is a useful descriptor for the change upon the approach of an electrophile, nucleophile, or radical reagent at the site k of the substrate. The second approach to the static-density response used in Part 1 came from a Kohn−Sham (KS) electron density model, which was expressed in terms of the KS one-electron density matrix $\gamma_S(\mathbf{r},\mathbf{r}')$ and a mean orbital difference $\Delta\epsilon$.[6] This less restrictive representation of the density response function led to the same expression (2), thereby

† Universitat Jaume I.
‡ Uppsala University.
§ Universitat de València.

10.1021/jp982801i CCC: $18.00
Published on Web 02/20/1999

showing that nonlocality was self-contained in the term incorporating the variations of the electronic chemical potential, promoted by the presence of reagents of variable hardness on the substrate. This nonlocal effect manifested itself, for the case of the reactivity of the cyanide ion, in the form of an intramolecular charge transfer (CT) between both reactive sites involved in this ambidented nucleophilic agent. One of the limitations of this formulation was the presence of a constant factor $s°(\mathbf{r})$ in eq 2, which appeared as the intrinsic local softness, in the absence of the perturbing potential. Moreover, as it is shown here, the reactivity of acetaldehyde enolate used as a test system is wrongly predicted by this elementary nonlocal approach.

The interest now is focused on describing the changes of local descriptors of site reactivity along a progress coordinate that helps introduce a variable softness factor.[7] This is achieved by adopting a Fukui response function as proposed by Fuentealba and Parr in the context of DFT.[7] Here, a more elaborated formulation is presented of nonlocal reactivity that incorporates second-order derivatives of the electron density and third derivatives of the electronic energy. The model is developed within a local approximation on the kernel $t(\mathbf{r},\mathbf{r}')$ of the function $t(\mathbf{r})$ defined by[7]

$$t(\mathbf{r}) = \left[\frac{\partial s(\mathbf{r})}{\partial N}\right]_{v(\mathbf{r})} \tag{3}$$

An important advantage of the present approach resides in its ability to include solvent effects in a natural way. Furthermore, for a given chemical mechanism having a definite transition structure (TS), this geometry provides a vantage point to sense the response to external perturbing potentials of the reactant with geometric arrangement reproducing the TS as much as possible. This leads to a new concept of a virtual TS to describe the results obtained from descriptors associated with higher order derivatives of the density with respect to either the particle number or the external potential. This virtual TS applies to isoelectronic series, and it is a region around the geometry of a leading TS.

The article is organized as follows. In Section 2, we derive general equations to represent the variations of the Fukui function to nucleophile, electrophile, or radical substrates, promoted by the approach of reagents of variable hardness. An approximate response function in the local regime is used to derive working formulas involving regional or condensed-to-atoms new reactivity indexes and the derivative of global softness. Section 3 contains an illustration of the methodology as it is applied to the reactivity of acetaldehyde enolate ion perturbed by two limiting model electrophiles, namely, a point charge simulating the attack to an enolate-like substrate at a virtual transition structure (VTS) and the attack to the same substrate by a ghost atom with a fractional nuclear charge, simulating a softer environment. By this procedure, we intend to explore the electronic propensity of the system to interconvert via one of the two possible (C-alkylated/O-alkylated) products, in terms of the variation of the Fukui function, in the vicinity of the VTS. Solvent effects are qualitatively discussed within the present model, and compared with experimental results. In Section 4, the predicted reactivity pattern, taking into account both model electrophiles and solvent effects, is checked against supermolecule calculations of the actual potential hypersurface containing the enolate ion plus the CH_3Cl alkylating agent. Solvent effects are estimated at the supermolecule level by introducing a discrete number of water molecules and calculating the different ground and transition structures. Our main conclusions are described in Section 6.

2. Theory

The Fukui function $f(\mathbf{r})$ appears in the DFT formulation when one writes the total differential of the electronic chemical potential, considered as a function on N and a functional of $v(\mathbf{r})$, $\mu = \mu[N,v(\mathbf{r})]$,[8] as

$$\mathrm{d}\mu = \left[\frac{\partial \mu}{\partial N}\right]_{v(\mathbf{r})} \mathrm{d}N + \int \mathrm{d}\mathbf{r}\left[\frac{\delta \mu}{\delta v(\mathbf{r})}\right]_N \delta v(\mathbf{r}) = 2\eta\, \mathrm{d}N + \int \mathrm{d}\mathbf{r}\, f(\mathbf{r})\, \delta v(\mathbf{r}) \tag{4}$$

where,[8]

$$\eta = \frac{1}{2}\left[\frac{\partial \mu}{\partial N}\right]_{v(\mathbf{r})} = \frac{1}{S} \tag{5}$$

and

$$f(\mathbf{r}) = \left[\frac{\delta \mu}{\delta v(\mathbf{r})}\right]_N = \left[\frac{\partial \rho(\mathbf{r})}{\partial N}\right]_{v(\mathbf{r})} = \frac{s(\mathbf{r})}{S} \tag{6}$$

are the global hardness and the Fukui function for the system, respectively.

Also, since $f = f[N,v(\mathbf{r})]$, we may write

$$\mathrm{d}f(\mathbf{r}) = \left[\frac{\partial f(\mathbf{r})}{\partial N}\right]_{v(\mathbf{r})} \mathrm{d}N + \int \mathrm{d}\mathbf{r}'\left[\frac{\delta f(\mathbf{r})}{\delta v(\mathbf{r}')}\right]_N \delta v(\mathbf{r}') \tag{7a}$$

and

$$\mathrm{d}f(\mathbf{r}) = t(\mathbf{r})\frac{\mathrm{d}N}{S} + \int \mathrm{d}\mathbf{r}'\, \mathrm{f}(\mathbf{r},\mathbf{r}')\, \delta v(\mathbf{r}') \tag{7b}$$

which introduce the local function $t(\mathbf{r})$ defined in eq 3. The Fukui response function $f(\mathbf{r},\mathbf{r}')$ may be defined as

$$f(\mathbf{r},\mathbf{r}') = \left[\frac{\delta f(\mathbf{r})}{\delta v(\mathbf{r}')}\right]_N = t(\mathbf{r},\mathbf{r}') - t(\mathbf{r})\, f(\mathbf{r}') \tag{8}$$

that corresponds to the negative of the Fuentealba−Parr response function.[7] This nonlocal quantity satisfies the normalization conditions for the Fukui function as we will show below and may also be expressed in terms of the $t(\mathbf{r})$ function and its kernel $t(\mathbf{r},\mathbf{r}')$ satisfying[7]

$$t(\mathbf{r}) = \int \mathrm{d}\mathbf{r}'\, t(\mathbf{r},\mathbf{r}') \tag{9}$$

The kernel $f(\mathbf{r},\mathbf{r}')$ is the basic quantity in the present model. It gives, according to definition 8, the desired variations of the Fukui function at point $\mathbf{r}$, when the system undergoes a change in the external potential at a different point $\mathbf{r}'$, promoted for instance by a local perturbation due to the presence of a reagent. This formulation also solves the problem of introducing a constant local softness factor to describe nonlocal reactivity based on the static density response function, as was the case of the previous formulation.[2] The major difficulty in handling the nonlocal function $f(\mathbf{r},\mathbf{r}')$ lies in the representation of the kernel $t(\mathbf{r},\mathbf{r}')$. To simplify things, we propose to introduce a local approximation to this quantity, namely,

$$t(\mathbf{r},\mathbf{r}') = A(\mathbf{r})\, \delta(\mathbf{r} - \mathbf{r}') \tag{10}$$

where $A(\mathbf{r})$ is any function that conserves the normalization condition

$$\int d\mathbf{r}\, \delta f(\mathbf{r}) = \delta \int d\mathbf{r}\, f(\mathbf{r}) = 0 \tag{11}$$

because $f(\mathbf{r})$ is normalized to unity. One of the possible functions satisfying condition 11 is the following:

$$A(\mathbf{r}) = f(\mathbf{r}) \left[\frac{\partial S}{\partial N}\right]_{v(\mathbf{r})} \tag{12}$$

The proof is straightforward yet very illustrative because it will allow us to introduce an additional equation for the function $t(\mathbf{r})$. Let us write the changes in the Fukui function produced by local changes in the external potential as follows:

$$df(\mathbf{r}) = \int d\mathbf{r}' \left[\frac{\delta f(\mathbf{r})}{\delta v(\mathbf{r}')}\right]_N \delta v(\mathbf{r}') = \int d\mathbf{r}'\, f(\mathbf{r},\mathbf{r}')\, \delta v(\mathbf{r}') \tag{13}$$

where the Fukui static response function $f(\mathbf{r},\mathbf{r}')$ has the form defined in eq 8. Now, introducing eqs 8, 10, and 12 into eq 13, and integrating over the $\mathbf{r}$ space, we find that condition 11 is fulfilled by the function $A(\mathbf{r})$, with the following additional condition for the function $t(\mathbf{r})$:

$$\int d\mathbf{r}\, t(\mathbf{r}) = \frac{\partial}{\partial N} \int d\mathbf{r}\, s(\mathbf{r}) = \left[\frac{\partial S}{\partial N}\right]_{v(\mathbf{r})} \tag{14}$$

which results directly from definition 3. With our approximate $t(\mathbf{r},\mathbf{r}')$ kernel defined by eqs 10 and 12 at hand, we may rewrite eq 7b as

$$df(\mathbf{r}) = A(\mathbf{r})\, \delta v(\mathbf{r}) - t(\mathbf{r}) \Delta\mu \tag{15}$$

which results after using eqs 8, 10, and 12 together with the identity[9]

$$\int d\mathbf{r}'\, f(\mathbf{r}') = \delta v(\mathbf{r}') = \Delta\mu - \frac{\Delta N}{S} \tag{16}$$

Let us comment on the structure of eq 15. The first term contains a complex variable coefficient for the changes in the electrostatic potential induced at any point $\mathbf{r}$ of the substrate by the presence of the reagent represented as an external potential. This contribution, which may be expected to be important in the long-range interaction regime, is associated with an electrostatic (namely *charge control*) contribution to the variations in the Fukui function, whereas the second one, which is proportional to the changes in the electronic chemical potential along the progress coordinate, may be associated with a contribution accounting for the degree of charge transfer that takes place during the chemical process.[8,9] This aspect of the present model may be clarified, by examining with further details the coefficients of the electrostatic factor $\delta v(\mathbf{r})$ and the electronic polarization $\Delta\mu$ contribution to $df(\mathbf{r})$.

Let us first focus on the variable coefficient $A(\mathbf{r})$. We may use eq 5 to write the derivative of the global softness with respect to the number of electrons as follows:

$$\left[\frac{\partial S}{\partial N}\right]_{v(\mathbf{r})} = \frac{\partial}{\partial N}\left[\frac{1}{\eta}\right]_{v(\mathbf{r})} = -3S^2\gamma \tag{17}$$

that introduces the γ-function of Fuentealba and Parr,[7] defined by

$$\gamma = \frac{1}{3}\left[\frac{\partial \eta}{\partial N}\right]_{v(\mathbf{r})} = \frac{1}{6}\left[\frac{\partial^3 E}{\partial N^3}\right]_{v(\mathbf{r})} \tag{18}$$

Multiplying both side of eq 17 by $f(\mathbf{r})$ and using eq 18, we obtain the desired result, namely,

$$A(\mathbf{r}) = -3S^2\gamma\, f(\mathbf{r}) \tag{19}$$

Useful formulas to evaluate the γ-function from first and second ionization potentials I_1 and I_2, and electron affinity A_1 are available from ref 7. For instance, introducing the approximation $I_n = nI_1$,[10] the following simple expression for the γ quantity is obtained:

$$\gamma = -c\eta = -\left[\frac{A_1}{3I_1 - A_1}\right]\eta \tag{20}$$

In those cases where the quantities I and A are not available from the experiment, we may still get estimates of them by using, for instance, Koopman's theorem. Under this approximation, we may write

$$c = \left[\frac{\epsilon_1}{\epsilon_1 - 3\epsilon_h}\right] \tag{21}$$

that introduces the one-electron orbital energies of the higher occupied (HOMO) and lowest unoccupied (LUMO) levels, ϵ_h and ϵ_l, respectively. Other definitions for the I and A quantities are possible. However, definition 21 reveals that c will be in general a positive definite quantity if the system presents unbound LUMO levels so that the γ quantity will give in general negative contributions to $A(\mathbf{r})$. On the other hand, the γ-function being a global property of the system, it follows from eq 19 that $A(\mathbf{r})$ may be expressed in a form condensed-to-atom or groups, as the Fukui function does.

Let us now focus on the second coefficient $t(\mathbf{r})$ of eq 15. Since this expression is satisfied at any point $\mathbf{r}_k$ in the molecular region, we may consider that it may have a regional or a condensed-to-atom expression and other local properties, as proposed by Yang and Mortier[11] and also by Geerlings et al.[12] For instance, on the basis of eq 3, we may write a finite difference formula for $t(\mathbf{r}_k)$ condensed to atom k as follows:

$$t_k^- = s_k(N) - s_k(N-1) \tag{22a}$$

and

$$t_k^+ = s_k(N+1) - s_k(N) \tag{22b}$$

for electrophilic and nucleophilic attacks, respectively.

Remembering the relationship between local softness and the Fukui function, namely, $s(\mathbf{r}) = f(\mathbf{r})S$, and using the finite difference expression for the Fukui function condensed to the k-th atom,[11,12] one gets

$$f_k^-(N) = \rho_k(N) - \rho k(N-1) \tag{23a}$$

and

$$f_k^-(N-1) = \rho_k(N-1) - \rho_k(N-2) \tag{23b}$$

where $\rho_k(N)$, $\rho_k(N-1)$ and $\rho_k(N-2)$ are the statistical electronic populations on atom k in systems with N, $(N-1)$ and $(N-2)$ electrons, respectively. Approximate expressions for the coefficients of $\Delta\mu$ in eq 15 may be written as follows:

$$t_k^- = S[\rho_k(N) - 2\rho_k(N-1) + \rho_k(N-2)] \tag{24a}$$

$$t_k^+ = S[\rho_k(N+1) - 2\rho_k(N) + \rho_k(N-1)] \tag{24b}$$

and

$$t_k^{\bullet} = \frac{1}{2}[t_k^- + t_k^+] \tag{24c}$$

for electrophilic, nucleophilic, and radical attacks, respectively.

For the specific case involving the reactivity of the enolate ion, which we shall examine in detail in the sections below, eq 15 takes the operational form condensed to atom *k*.

$$\Delta f_k^- = A_k^- \, \delta v_k - t_k^- \delta\mu \tag{25}$$

with

$$A_k^- = -3S^2\gamma[\rho_k(N) - \rho_k(N-1)] \tag{26}$$

and t_k^- is given by eq 24a.

We may now comment on the physical nature of the contributions to the fluctuation of the Fukui function, upon the approach of the reacting system along a progress coordinate leading to a geometry resembling the TS. The first contribution, both in eqs 15 and 25, to the extent that the variations in the external potential reflect electrostatic factors, collects from $A(\mathbf{r})$, the global reactivity index, and responses associated with ionic interactions. The second contribution to $df(\mathbf{r})$ is proportional to the change in the electronic chemical potential, a global index that drives the direction and amount of charge transfer for a chemical reaction.[8] Therefore, the second contribution, as modulated by the derivative of local softness (i.e., a polarizability parameter of the system at a given site in a molecule), should be more likely related to short-range electronic polarization effects.

Solvent effects can be rationalized as external potential effects on the molecular charge density. Let us first stress the point that, in polar solvents, the driving force governing the changes in Δf_k^- induced by solvation will be dominated by the electrostatic contribution (first term of eq 25). If we assume that the quantities A_k^- and t_k^- will be not significantly changed by the solute−solvent interactions, we may write the following approximate expression for the variation (δ_s) due to the solvent:

$$\delta\Delta_s f_k^- \cong A_k^- \delta\delta v_{sk} - t_k^- \delta\Delta\mu_s \tag{27}$$

However, Pearson[27] has reported an important result showing that electronegativity (i.e., $-\mu$) is mostly unaffected by solvation. This means that the term $t_k^- \delta\Delta\mu_s$ will not give significant contributions to $\delta\Delta_s f_k^-$ in eq 27. On the other hand, the first term of eq 27 may be approached as follows:[28]

$$A_k^- \, \delta_s \, \delta v_k \cong -\left(1 - \frac{1}{\epsilon}\right) A_k^- \, \delta v_k \tag{28}$$

which leads to

$$\delta_s \, \Delta f_k^- \cong -\left(1 - \frac{1}{\epsilon}\right) A_k^- \, \delta v_k \tag{29}$$

as an approximate expression for the changes in the Fukui function variation when the system is moved from the gas to the solution phase; ϵ is the macroscopic dielectric constant of the medium, and δv_k is the change in electrostatic potential in the gas phase.

3. Gas-Phase Reactivity of the Acetaldehyde Enolate toward Model Electrophiles of Variable Hardness

It is widely recognized that alkylations of enolates are synthetically valuable and mechanistically intriguing processes.[13,14] Several hypotheses have been advanced to pinpoint the factors controlling the ratios of C-alkylation to O-alkylation and the stereoelectronic factors governing the direction of attack on the enolate by the alkylating agent.[15,22] For instance, the introduction of metallic counterions into the substrate may favor either C- or O-alkylation by forming ion pair intermediates.[15,17] Solvent effect is also recognized as a determining factor controlling the kinetic products of alkylation.[18,19] The nature of the electrophilic agent may also play a relevant role in the alkylation reaction of enolates.[20] Therefore, the alkylation reactions of this system may take place either at the α-carbon or at the oxygen atoms, depending on the medium conditions and the nature of the alkylating (hard/soft) agent.[20] In polar solvents, the preferential solvation of the oxygen atom leaves the α-carbon as the active site for alkylation.[21] While solvent effects upon enolate ion chemistry have been extensively studied,[18,19] the effect coming from the electronic nature of the alkylating agent has received less attention. The theoretical model of pair-site reactivity allows for an analysis of both the electronic effect promoted by the presence of electrophilic agents of variable hardness and solvent effects.

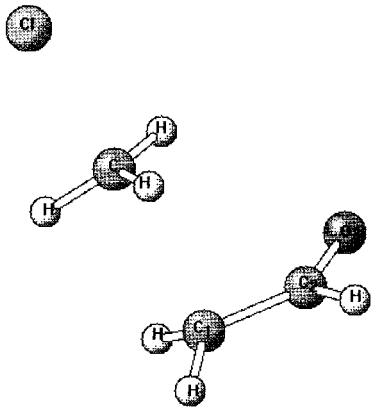

Figure 1. Calculated transition structure for the C-alkylation channel.

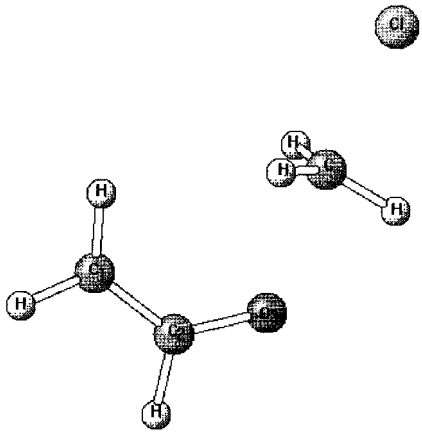

Figure 2. Calculated transition structure for the O-alkylation channel.

Figures 1 and 2 show the calculated transition structures for the C- and O-alkylation reactions of acetaldehyde enolate with CH_3Cl, respectively. These structures were obtained at the HF/6-31G* level of the theory [23,24] (further details in Section 4). The first factor to be considered in the alkylation reaction of acetaldehyde enolate was the nature of the electrophilic agent E^+. Two limiting electrophiles models are considered. The first one considers the approach of a point charge (PC) (as a model for an infinitely hard E^+) from large distance (infinity) to the position of a virtual transition structure (VTS), corresponding to the TS geometry for the O-channel, which resulted to be the one with the lowest activation energy (see Section 4 for details).

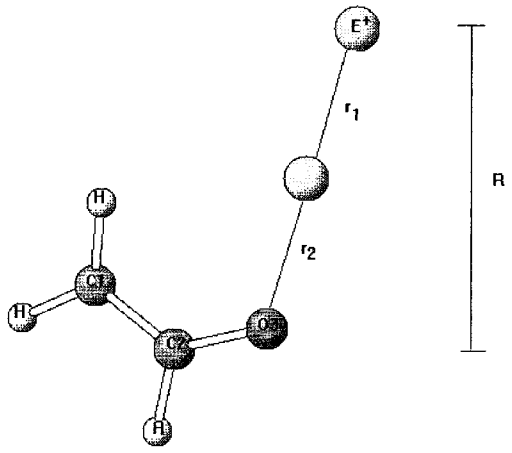

Figure 3. Virtual transition structure considered for the interaction of the TS−O structure with model electrophiles. Relevant geometrical parameters are included. The progress coordinate X is defined as $X = (r_1 - r_2)/R$. See the text for further details.

The VTS geometry is depicted in Figure 3, and it was defined by taking out the chlorine atom and by replacing the methyl cation by a hole where the PC is to be placed at the end of the virtual process. In this way, as the real system converges toward the saddle point of index one, the electron density is expected to converge into the one defining the TS. Thus, by using the geometric arrangement for the reactant that corresponds to the one it should have in the TS, we obtain a calculated electron density that is expected to contain the major information about the external potential at the transition structure. As the external potential has not all the electronic properties of the companion molecule, it is useful to employ the term virtual transition state. In the present case, we have taken a PC having a net charge equal to that of the carbon of the CH_3^+ group at the TS, shown in Figure 2. This value was about 0.47 e units. The second E^+ model, consists of forming a pseudoatom (PA) by adding orbitals to the PC. By this procedure, we intended to mimic some degree of electronic polarizability on the softer electrophile PA. Both model reagents were allowed to approach the VTS structure along a progress coordinate X, defined in Figure 3.

In the case of an infinitely hard electrophile model, RHF/6-31G*[23,24] calculations were performed on the system formed by the enolate ion, with a VTS geometry for the selected progress coordinate ranging from $X = 0.21-0.0$. For each point, the quantities A_k^-, t_k^-, $\delta\nu_k$, $\Delta\mu$ were evaluated using eqs 26 and 24a for the first two. The variations in the electrostatic potential at site k were approached as follows. We first evaluated the electrostatic potential at that site in the presence of the PC as

$$\nu_k = \sum_{l \neq k} \frac{Q_t}{|\mathbf{r}_k - \mathbf{r}_l|} \tag{30}$$

where Q_l is the net charge of the atoms (including the PC) located at $\mathbf{r}_l$. Next, we defined the variation $\delta\upsilon_k = \upsilon_k - \upsilon^\circ_k$, where υ°_k is the electrostatic potential at long distance ($X > 0.21$). The changes in electronic chemical potential were obtained by taking the differences of μ using the same protocol followed to approach $\delta\upsilon_k$. The electronic chemical potential was obtained from the approximate formula[8]

$$\mu \approx \frac{\epsilon_h + \epsilon_l}{2} \tag{31}$$

in terms of the one-electron energies of the HOMO and LUMO levels.

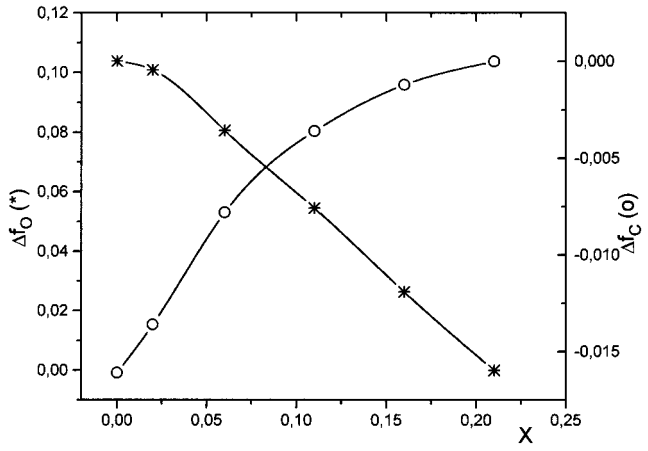

Figure 4. Predicted fluctuations of the Fukui function from eq 25 at the carbon (○) and the oxygen (*) sites, promoted by the interaction of the acetaldehyde enolate and PC (infinitely hard) electrophile model.

TABLE 1: Reactivity Indexes and Partition of Δf_k for the O Reaction Channel Perturbed by a PC Model Electrophile

X	A_k^-	t_k^-	$\delta\nu_k$	$\Delta\mu$	$\Delta f^-_k = A^-_k\,\delta\nu_k - t^-_k\,\Delta\mu$		
0.21	2.2373	0.7839	0.0000	0.0000	0.0000	0.0000	0.0000
	2.9417	−0.5039	0.0000	0.0000	0.0000	0.0000	0.0000
0.16	2.1303	0.7627	0.0102	−0.0062	0.0264	0.0217	−0.0047
	2.8363	−0.5107	0.0007	−0.0062	−0.0012	0.0020	0.0032
0.11	1.9979	0.7247	0.0224	−0.0134	0.0545	0.0448	−0.0097
	2.7117	−0.5172	0.0012	−0.0134	−0.0036	0.0033	0.0069
0.006	1.8239	0.6342	0.0366	−0.0218	0.0806	0.0668	−0.0138
	2.5872	−0.5141	0.0013	−0.0218	−0.0078	0.0034	0.0112
0.02	1.6088	0.5016	0.0530	−0.0311	0.1009	0.0853	−0.0156
	2.4475	−0.5081	0.0009	−0.0311	−0.0136	0.0022	0.0158
0.0[a]	1.5218	0.4400	0.0582	−0.0347	0.1039	0.0886	−0.0153
	2.3961	−0.5039	0.0006	−0.0347	−0.0160	0.0014	0.0175

[a] The value $X = 0.0$ corresponds to the VTS. See the text for details and definitions. All quantities are in atomic units. First entry corresponds to k = oxygen (O3); second entry corresponds to k = α-carbon (C1).

With all these quantities at hand, one may then evaluate the changes in the Fukui function, according to eq 25, for the approach of an infinitely hard model electrophile. The results are depicted in Figure 4. There, the variations in the Fukui function at the oxygen site show an increasing pattern from a long-range interaction regime to the TS−O, $\Delta f_O^- > 0$; whereas the variation of the Fukui function at the carbon site shows the opposite trend $\Delta f_C^- < 0$. In other words, $\Delta f_O^- > 0$ implies that the Fukui function at the final state (TS−O) is larger than the corresponding Fukui function at the beginning of the reaction. The Fukui functions for both the C1 and O3 sites in acetaldehyde enolate isolated were $f^\circ_{C1} = 0.55$ and $f^\circ_{O3} = 0.42$, showing that the O reaction channel does not lead to the correct kinetic control product.[21,22] The origin of the inversion in the Fukui function at the TS−O may be traced back to an intramolecular charge transfer between the two active sites of acetaldehyde enolate.[25] This conclusion follows from the fact that no fluctuations were observed in the electronic properties at the passive carbon C2. Therefore, eq 25 brings the reactivity analysis one step further than the static reactivity picture developed around the electronic structure of the ground state of reagents. Second, it provides a partitioned picture of the fluctuation in the Fukui function in terms of electrostatic (charge control), driven by changes in the electrostatic potential, and nonelectrostatic (charge transfer) contributions, driven by the changes in the electronic chemical potential.

Table 1 summarizes the different contributions to Δf_k^-, for selected values of the progress coordinate X. This table also

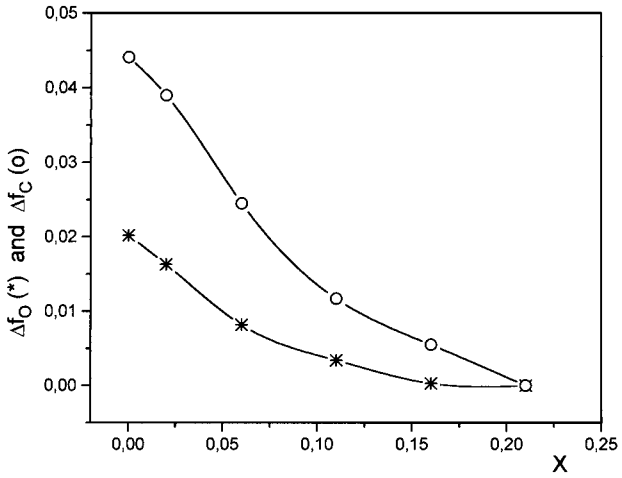

Figure 5. Predicted fluctuations of the Fukui function from eq 25 at the carbon (○) and the oxygen (*) sites, promoted by the interaction of the acetaldehyde enolate and PA (soft) electrophile model.

TABLE 2: Reactivity Indexes and Partition of Δf_k for the O Reaction Channel Perturbed by a Pseudoatom Model Electrophile

X	A_k^-	t_k^-	δv_k	$\Delta\mu$	$\Delta f^-_k = A^-_k\,\delta v_k - t^-_k\,\Delta\mu$		
0.21	0.4283	0.7627	0.0000	0.0000	0.0000	0.0000	0.0000
	0.5690	−0.4910	0.0000	0.0000	0.0000	0.0000	0.0000
0.16	0.4927	0.7478	0.0093	0.0050	0.0003	0.0040	0.0037
	0.6609	−0.5084	0.0040	0.0050	0.0055	0.0030	−0.0025
0.11	0.5650	0.7148	0.0200	0.0111	0.0034	0.0113	0.0079
	0.7715	−0.5236	0.0099	0.0111	0.0117	0.0076	−0.0041
0.06	0.6508	0.6900	0.0323	0.0186	0.0082	0.0210	0.0128
	0.9066	−0.5426	0.0159	0.0186	0.0245	0.0144	−0.0101
0.02	0.7436	0.6650	0.0465	0.0275	0.0163	0.0346	0.0183
	1.0624	−0.5559	0.0223	0.0275	0.0390	0.0237	−0.0153
0.0[a]	0.7781	0.6578	0.0520	0.0309	0.0202	0.0405	0.0230
	1.1223	−0.5601	0.0239	0.0309	0.0441	0.0268	−0.0173

[a] The value $X = 0.0$ corresponds to the VTS. See the text for details and definitions. All quantities in atomic units. First entry corresponds to k = oxygen (O3); second entry corresponds to k = α-carbon (C1).

contains all the information concerning the reactivity parameters A_k^- and t_k^-, together with the variations of the electrostatic and electronic chemical potentials. We may first observe that the electrostatic contributions δv_k at the oxygen atom (first entry of Table 1) are significantly greater than the corresponding variations at the α-carbon atom (second entry). Therefore, along the O reaction channel, the interaction of an infinitely hard model electrophile (PC) will favor alkylation at the oxygen site as the kinetic control product, in agreement with a local hard and soft acid and base (HSAB) principles. The variations in the electronic chemical potential, as defined in the present approach, contribute with the same quantity to both O and α-C sites and to the nonelectrostatic (electronic polarization) component of Δf_k^-. However, the electronic polarization contribution may be analyzed through the reactivity index t_k^- of eq 25. This new reactivity descriptor gives, according to eq 3, the variations of the local softness with respect to the electron transfer. From Table 1, it may be observed that at the oxygen site, the variation in t_k^- gives non-negative contributions to Δf_k^-. This means that, along the progress coordinate, the local softness at the VTS will be lower than the local softness at the oxygen site at the beginning of the reaction. One may then argue, on the basis of the relationship between local softness and hardness proposed by Fuentealba,[26] that the lower the softness, the higher is the hardness at a given site. Therefore, the electrostatic contribution will still dominate the changes in the Fukui function at the oxygen site through the positive fluctuations of the t_k^- index.

On the other hand, the changes in the reactivity index t_k^- at the α-carbon (C1) give negative contributions to Δf_k^- along the whole progress coordinate X. An analysis similar to that used above, for the variations of t_k^- at the oxygen site, shows that the approach of an infinitely hard electrophile renders the α-carbon softer than it is at the beginning of the reaction.

The analysis of the gas-phase reactivity pattern of the acetaldehyde enolate toward attack by a softer model electrophile (PA) is summarized in Figure 5. In this case, no inversion in the Fukui function is observed with reference to the isolated enolate system. This result indicates that acetaldehyde enolate would be less selective along the O reaction channel toward soft electrophiles and the static reactivity picture would suffice to explain reactivity under these circumstances. In other words, we may conjecture that, in the presence of a soft electrophile, acetaldehyde enolate would yield a significant amount of C-alkylated kinetic products. The partitioned analysis reveals that the α-carbon site becomes more reactive at the VTS geometry (see Figure 5). The positive variations in Δf_k^- for both the C1 and O3 sites may be explained by the contributions of $A_k^-\delta v_k$ and $t_k^-\Delta\mu$, summarized in Table 2. For the O site, both terms give positive contributions to Δf_{O3}^-. This increase follows from the fact that δv_k contributions are significantly higher than the electronic polarization term all along the progress coordinate X. On the other hand, the positive fluctuations in Δf_{C1}^- follow from a cooperative effect that results from the negative contributions of $t_{C1}^-\Delta\mu$ to Δf_{C1}^-, along the X coordinate.

3.1. Solvent Effects. It is well-known that the reaction of enolate ions with methyl chloride in the gas phase takes place via an O attack to produce methyl vinyl ethers.[23,24] However, when the reaction is carried out in polar solvent solution, the main product corresponds with the C attack.[24] We will show that eq 25 may also be used in an approximate context to qualitatively explain the changes in the reactivity pattern from the gas to the solution phase, considering both the O reaction and C reaction channels. This analysis may be performed by introducing some approximations, as well as empirical results reported by Pearson[27] concerning the solvent effects on the electronic chemical potential and related quantities.

Using the value $\epsilon = 80.0$ to simulate water polarity and the intrinsic values of A_k^- and δv_k, quoted in Table 1, the results obtained from eqs 28 and 29 are depicted in Figure 6. It may be seen that while the Δf_{C1}^- remains unaffected by solvation, the oxygen site shows a significant decrease in the Δf_k^- index. Furthermore, because δ_s, $\Delta f_O^- < 0$, all along the progress coordinate, one may conclude that the solvent effect will make the oxygen atom less reactive at the VTS geometry. Therefore, eq 25 may be used in an approximate way to qualitatively predict the changes in the observed reactivity pattern from the gas to the solution phase in the acetaldehyde enolate alkylation reaction.

4. Transition Structure Reactivity from the Full Potential Energy Surface

The results reported above were calculated with the equations derived in Section 2. The agreement with experimental information is an encouraging point. Of general interest for present day computing approaches to chemical reactivity is the testing with supermolecule calculations offering a complementary view. For

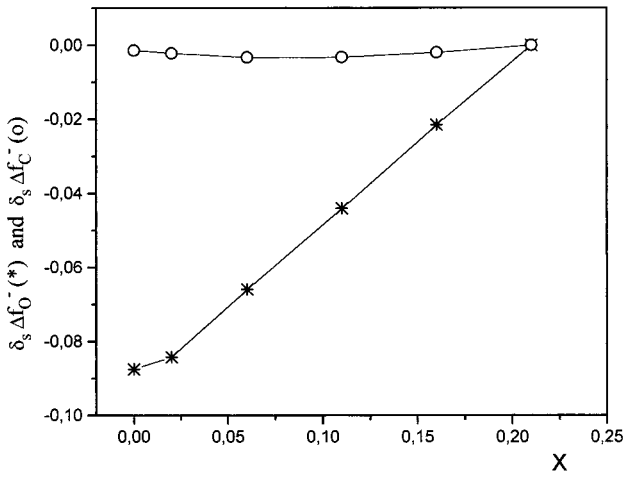

Figure 6. Predicted fluctuations of the Fukui function from eq 31 at the carbon (○) and the oxygen (*) sites, in a simulated aqueous medium, for the interaction of the acetaldehyde enolate and a PC (infinitely hard) electrophile model.

the system herein studied, supermolecule calculations can be carried out including actual determination of the transition structure.

In Tables 3 and 4, the relative energies of the stationary points, the chemical electronic potential μ, the chemical softness S, and the values of the Fukui function on C1 and O3 centers, f_{C1}^- and f_{O3}^-, respectively, along the reactive pathways of both processes including the transition structures TS−C and TS−O are presented along with the two alternative reactivity pathways. Both reactive channels are exothermic processes and gas-phase as well as solution results show that the C-alkylated product, propenaldehyde, is more stable than the O-alkylated product, methyl vinyl ether.[23,24] In agreement with experimental data, the transition structure corresponding to the attack at the oxygen atom, TS−O, is more stable (3.2 kcal/mol) than the transition structure of the carbon atom attack, TS−C, and consequently, methyl vinyl ether is the product of kinetic control. The lengths of the C1−C4 and O3−C4 forming bonds at TS−C and TS−O are 2.491 and 2.136 Å, respectively, with the latter TS being more advanced. The C4−C1−C2 bond angle at the TS−C is 96.2°, while the C4−O3−C2 bond angle at TS−O is 121.2°. These bond angles are held frozen along the approach of CH_3-Cl to the enolate system, simulating both reactivity pathways.

Remembering that the values of the Fukui functions f_{C1}^o and f_{O3}^o for the enolate isolated system are 0.55 and 0.42, respectively, for an electrophilic reaction, the C1 center is accordingly predicted to be more reactive than the O3 center. Unfortunately, this result does not correspond with the fact that the reaction pathway via TS−O is more energetically favorable than that via TS−C. In the analysis based on eq 25, it was shown that the conclusions drawn from this static reactivity pattern are drastically a function of the progress coordinate X. Keeping all the geometrical parameters that are not involved in the definition of X frozen, the variations of A_k^-, t_k^-, and f_k^-, along the reactivity pathways of both processes can be monitored.

An analysis of the results show that the f_{C1}^- and f_{O3}^- values along the C reaction channel are ca. 0.5 and 0.4, respectively, from $X = 0.14$ to $X = 0.0$ (see Table 3). An opposite result is obtained when the Fukui functions are calculated at the transition structures TS−O. At the transition structure TS−C ($r_2 = 2.491$ Å), these values are similar to those of the acetaldehyde enolate isolated (f_{C1}^- and f_{O3}^- are 0.50 and 0.30, respectively), while for the transition structure TS−O, ($r_2 = 2.136$ Å), there is an inversion of the corresponding values (f_{C1}^- and f_{O3}^- are 0.33 and 0.50, respectively), showing that the O3 center is more reactive. In other words, the preference for one reactive channel is decided

TABLE 3: Total and Relative Energies, Electronic Chemical Potential μ, Chemical Softness S, and Values of the Fukui Function at C1 and O3, along the C Reaction Channels

X	0.0	0.02	0.06	0.10	0.14
HF (a.u.)	−651.380120	−651.383506	−651.388605	−651.391260	−651.392162
ΔE (kcal/mol)	7.56	5.43	2.23	0.57	0.00
HOMO	−0.1100	−0.0847	−0.0792	−0.0762	−0.0739
LUMO	0.2919	0.3313	0.3325	0.3282	0.3223
ρ_{C1}	6.4640	6.5010	6.5080	6.5122	6.5163
ρ_{O3}	8.7033	8.7556	8.7672	8.7715	8.7740
ρ_{C1} (N − 1)	5.9686	5.9685	5.9653	5.9630	5.9615
ρ_{O3} (N − 1)	6.4021	8.4011	8.4005	8.3999	8.3996
μ	0.09	0.12	0.13	0.13	0.12
S	4.98	4.81	4.86	4.94	5.05
f_{Cl}^-	0.50	0.53	0.54	0.55	0.55
f_{O3}^-	0.30	0.35	0.37	0.37	0.37

TABLE 4: Total and Relative Energies, Chemical Potential μ, Chemical Softness S, and Values of the Fukui Function at C1 and O3 along the O Reaction Channels

X	0.0	0.02	0.06	0.11	0.16	0.21
HF (a.u.)	−651.385211	−651.386516	−651.392748	−651.396049	−651.396801	−651.396089
ΔE (kcal/mol)	6.92	6.10	2.19	0.12	−0.35	0.09
HOMO	−0.1198	−0.1017	−0.0867	−0.0807	−0.0768	0.0737
LUMO	0.3195	0.3436	0.3518	0.3466	0.4061	0.3311
ρ_{C1}	6.4181	6.4518	6.4794	6.4906	6.4979	6.5037
ρ_{O3}	8.7941	8.7983	8.8001	8.8010	8.8022	8.8037
ρ_{C1} (N − 1)	6.0858	6.1032	6.1119	6.1160	5.9475	5.9498
ρ_{O3} (N − 1)	8.2894	8.2725	8.2615	8.2570	8.4117	8.4117
μ	0.10	0.12	0.13	0.13	0.16	0.13
S	4.55	4.49	4.56	4.68	4.14	4.94
f_{C1}	0.33	0.35	0.37	0.37	0.55	0.55
f_{O3}	0.50	0.53	0.54	0.54	0.39	0.39
Δf_{Cl}^-	−0.22	−0.20	−0.18	−0.18	0.00	0.00
Δf_{O3}^-	0.13	0.15	0.16	0.17	0.01	0.00

TABLE 5: Chemical Potential, μ, Chemical Softness, S, and Values of the Fukui Function for the Enolate·2H_2O, TSC·2H_2O, and TSO·2H_2O

	enolate·2H_2O	TSC·2H_2O	TSO·2H_2O
HOMO	−0.1074	−0.1564	−0.1776
LUMO	0.3829	0.2579	0.2976
ρ_{C1}	6.4116	6.3852	6.3045
ρ_{O3}	8.8292	8.7357	8.8271
$\rho_{C1}(N-1)$	5.9071	5.9337	5.8557
$\rho_{O3}(N-1)$	8.4810	8.4769	8.4956
μ	0.14	0.05	0.06
S	4.08	4.83	4.21
f^-_{Cl}	0.50	0.45	0.45
f^-_{O3}	0.35	0.26	0.33

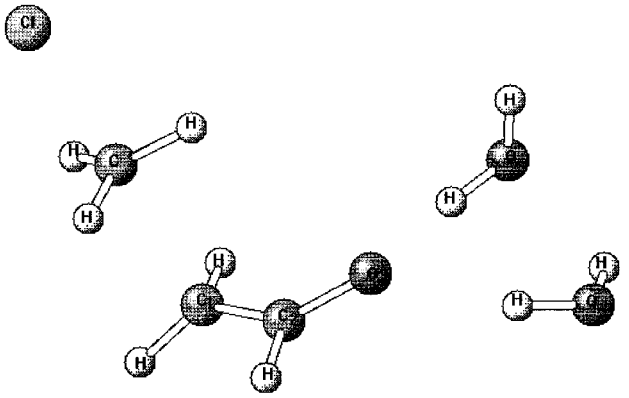

Figure 7. Calculated transition structure for the C-alkylation channel, including two water molecules to mimic solvation.

at the corresponding transition structure, and the analysis of the Fukui function values agrees well with the energetic arguments.

Along the O reaction channel (see Table 4 and Figure 2), the behavior of the Fukui functions is different. For X coordinate values between 0.10 and 0.02, f^-_{C1} and f^-_{O3} are ca. 0.4 and 0.5, respectively, showing that, in this range of the progress coordinate, the O3 center presents a larger value for the Fukui function. This inversion takes place at $X = 0.16$, where the potential energy surface presents a minimum corresponding to a reactant-like complex. This fact explains the change of the Fukui function at the O3 center in the transition structure TS−O, and in the gas phase, the electrophilic attack yields the O-alkylated kinetic product.

To analyze the reactivity in the solution phase, we have modeled the process in an aqueous environment, solvating the oxygen atom of the enolate system with two water molecules through hydrogen bonding interaction between the O3 atom and one hydrogen of the water molecule. Table 5 presents the values of the Fukui function for the enolate·2H_2O, TSC·2H_2O, and TSO·2H_2O, while Figures 7 and 8 show the geometries of the transition structures TSC·2H_2O, and TSO·2H_2O, associated with the C- and O-alkylation channels, respectively. This study shows that the inclusion of solvent effects in the isolated enolate ion does not modify the relative values of the Fukui function on the C1 and O3 centers, revealing that the C1 center is more reactive than the O3. In the solvated transition structures TSC·2H_2O, and TSO·2H_2O, the value of the Fukui function is larger in C1 than in O3 (see Table 5). These theoretical results are in agreement with the experimental results, which show that, in the solution phase, the C attack is preferred as the kinetic product in the solution phase.[24] Therefore, the calculated changes in the Fukui function, in both the gas and solution phase, correctly explain the reactivity of the acetaldehyde enolate in the vicinity of the corresponding transition structures, in complete agreement

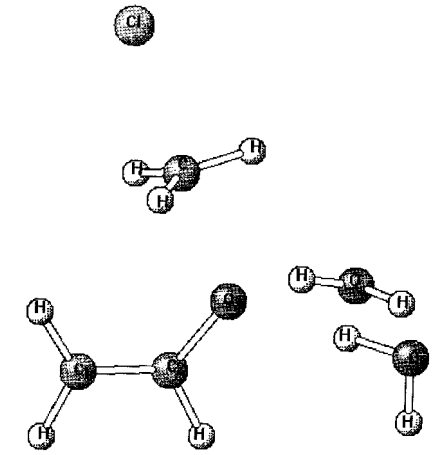

Figure 8. Calculated transition structure for the O-alkylation channel, including two water molecules to mimic solvation.

with the predicted reactivity pattern derived from our model eq 25, discussed in Section 3.

5. Summary of Approximations

This work presents an attempt to elaborate a theoretical framework to discuss pair site reactivity. Several approximations are involved in the derivation of our working eq 25, and we shall discuss them here.

(a) As correctly quoted by a referee, our expression (8) defining the second-order response function $f(\mathbf{r},\mathbf{r}')$ is not exact. This can be shown by directly taking the negative of the derivative of the first-order response function defined in eq 1 at constant external potential. From this results

$$f(\mathbf{r},\mathbf{r}') = -\left[\frac{\partial\chi(\mathbf{r},\mathbf{r}')}{\partial N}\right]_{v(\mathbf{r})} = \left[\frac{\partial s(\mathbf{r},\mathbf{r}')}{\partial N}\right]_{v(\mathbf{r})} - \frac{\partial}{\partial N}[s(\mathbf{r})f(\mathbf{r}')] = t(\mathbf{r},\mathbf{r}') - t(\mathbf{r})f(\mathbf{r}') - s(\mathbf{r})\left[\frac{\partial f(\mathbf{r}')}{\partial N}\right]_{v(\mathbf{r})} \quad (32)$$

where

$$t(\mathbf{r},\mathbf{r}') = \left[\frac{\partial s(\mathbf{r},\mathbf{r}')}{\partial N}\right]_{v(\mathbf{r})} \quad (33)$$

Note that eq 33 is consistent with the condition given in eqs 3 and 9. To prove this, just integrate eq 33 over the $\mathbf{r}'$ space coordinate and use

$$s(\mathbf{r}) = \int d\mathbf{r}'\, s(\mathbf{r},\mathbf{r}') \quad (34)$$

Also, eq 32 does satisfy the normalization condition $\int d\mathbf{r}'\, f(\mathbf{r},\mathbf{r}) = 0$. Equation 32 is an exact expression for the Fukui function kernel. Our proposal for $f(\mathbf{r},\mathbf{r}')$ given in eq 8 takes into account the first two terms of eq 32, and in this sense, it is an approximate expression for $f(\mathbf{r},\mathbf{r}')$. The neglect of the nonlocal (third) term in eq 32 may be only justified for an explicit expression of $t(\mathbf{r},\mathbf{r}')$, beyond the local approximation made in eq 10.

(b) The second main approximation involved in the present model is the local approximation made on the kernel $t(\mathbf{r},\mathbf{r}')$. This approximation is similar to that introduced by Vela and Gázquez[5] to represent the softness kernel. Certainly, this kind of approximation, though useful, is not exact. However, in the absence of accurate representations of these nonlocal quantities, they may be used to qualitatively represent the changes in electron density and its first derivatives with respect to the

number of electrons. We expect the local approximation on $t(\mathbf{r},\mathbf{r}')$ to asses the essential information contained in this quantity.

(c) Finally, a third approximation concerning electrostatic solvent effects made in eq 27 is based on the experimental results reported by Pearson.[27] In that work, it was shown that the electronegativity (i.e., electronic chemical potential) remains approximately invariant when passing from the gas to the solution phase.

6. Concluding Remarks

A pair site reactivity model derived from second-order static density response function has been developed. The formalism provides a simple expression, namely, eq 25, to help analyze the changes of the Fukui function induced by the presence of an electrophilic agent in a model ambident nucleophile. New reactivity indexes have been derived; they involve first derivatives of chemical hardness with respect to the total number of electrons (third-order derivatives with respect to the electronic energy) and local indexes accounting for the changes in local softness with respect to charge transfer. The model represented by eq 25 qualitatively reproduces the results obtained from a full calculation of the potential energy surface. They agree well with the observed reactivity pattern of acetaldehyde enolate toward alkylation by electrophiles of variable hardness. In the gas phase, the O reaction channel is correctly predicted as the product of kinetic control, in agreement with the experimental data. In the solution phase, the C-alkylation is predicted as the main product of kinetic control, as a consequence of a strong electrostatic solute−solvent interaction at the O site, which makes the Fukui function significantly decrease at this site thereby transferring the reaction control to the α-carbon site (i.e., *activation* at the α-carbon is predicted to occur by preferential solvation at the O site). This result stresses the nonlocal character of the reactivity pattern shown by acetaldehyde enolate in the gas and solution phases.

The analyses of the reactivity indexes are based upon the densities characterizing the transition structures of the different mechanisms. This introduces the concept of a reactivity path (to distinguish from the more mechanical concept of reaction paths or trajectories); the way the transition structure is populated is not an issue for reactivity studies, yet the necessary and sufficient condition for a mechanism to happen appears to be the population of the TS. Furthermore, the introduction of the idea of virtual transition structure allows for a modeling of one of the reactants as if it were wrapped with its electron density at the TS. This is perhaps not totally justified on theoretical grounds, but it turned out to be an excellent starting point to study general reactivity trends for the model system chosen here to test the more general reactivity indexes. The supermolecule calculations confirmed such trends.

Acknowledgment. This work has received financial support from FONDECYT, under Contracts 1970212 and 4980017. R.C. is indebted to Fundación Andes, Project C-13222/3 for financial support. P.P. is grateful to Departamento de Postgrado y Postítulo, PG/06/97, Universidad de Chile. R.C. and P.P. acknowledge support from the Departament de Ciènces Experimentals, Universitat Jaume I and the Department of Physical Chemistry, Uppsala University. O.T. gratefully acknowledges NFR for financial support. The authors are grateful to the Centre d'Informática de la Universitat Jaume I for providing them with CPU time on its HP9000/730 facilities.

References and Notes

(1) Shaik, S. S.; Schlegel, H. B.; Wolfe, S. *Theoretical aspects of physical organic chemistry;* Wiley: New York, 1992.

(2) Contreras, R.; Andrés, J.; Pérez, P.; Aizman, A.; Tapia, O. *Theor. Chem. Acc.* **1998**, *99*, 183.

(3) Berkowitz, M.; Parr, R. G. *J. Chem. Phys.* **1988**, *88*, 2554.

(4) Pérez, P.; Contreras, R.; Aizman, A. *Chem. Phys. Lett.* **1996**, *260*, 236.

(5) Vela, A.; Gázquez, J. L. *J. Am. Chem. Soc.* **1990**, *112*, 1490.

(6) Fuentealba, P.; Savin, A. Private communication. We thank these authors for making available to us their results prior to publication.

(7) Fuentealba, P.; Parr, R. G. *J. Chem. Phys.* **1991**, *94*, 5559.

(8) Parr, R. G.; Yang, W. In *Density Functional Theory of Atoms and Molecules*; Breslow, R., Goodenough, J. B., Halpern, J., Rowlinson, J. S., Eds.; The International Series of Monographs on Chemistry; Oxford Science Publications: New York, 1989.

(9) Gázquez, J. L. In *Structure and Bonding: Chemical Hardness*; Sen, K. D., Ed.; Springer-Verlag: New York, 1993; Vol. 80, p 27.

(10) March, N. H. *J. Chem. Phys.* **1982**, *76*, 1869.

(11) Yang, W.; Mortier, W. J. *J. Am. Chem. Soc.* **1986**, *108*, 5708.

(12) De Proft, F.; Langenaeker, W.; Geerlings, P. *Int. J. Quantum Chem.* **1995**, *55*, 459.

(13) Hoye, T. R.; Crawford, K. B. *J. Org. Chem.* **1994**, *59*, 520.

(14) Sprules, T. J.; Lavallée, J. F. *J. Org. Chem.* **1995**, *60*, 5041.

(15) Gareyev, R.; Ciula, J. C.; Streitwieser, A. *J. Org. Chem.* **1996**, *61*, 4589.

(16) Hatanaka, M.; Park, O. E.; Ueda, I. *Tetrahedron Lett.* **1990**, *31*, 7631.

(17) Hou, Z.; Yoshimura, T.; Wakatsuki, Y. *J. Am. Chem. Soc.* **1994**, *116*, 11169.

(18) Shirodkar, S.; Nerz-Stormes, M.; Thonton, E. R. *Tetrahedron Lett.* **1990**, *33*, 4699.

(19) McCarrier, M. A.; Wu, Y. D.; Houk, K. N. *J. Org. Chem.* **1993**, *58*, 3330.

(20) Duhamel, P.; Cahard, D.; Poirier, J. M. *J. Chem. Soc., Perkin Trans.* **1993**, *1*, 2509.

(21) Jones, M. E.; Kass, S. R.; Filley, J.; Barkley, R. M.; Ellison, G. B. *J. Am. Chem. Soc.* **1985**, *107*, 109.

(22) Houk, K. N.; Paddon-Row, M. N. *J. Am. Chem. Soc.* **1986**, *108*, 2659.

(23) Unless otherwise specified, all geometries of the transition structures have been fully optimized at the restricted Hartree−Fock (RHF) level with the 6-31G* basis sets. Electron density for the different atoms that are needed to evaluate the regional (local) reactivity indexes, A_k^-, t_k^-, and f_k^-, have been obtained from the atomic Mulliken population with hydrogens summed into heavy atom, for the different stationary points along a progress coordinate, for the systems with N, $N-1$, and $N-2$ electrons (charges: -1, 0, and $+1$, respectively).

(24) Frisch, M. J.; Trucks, G. W.; Schlegel, H. B.; Gill, P. M. W.; Johnson, B. G.; Robb, M. A.; Cheesman, J. R.; Keith, T.; Petersson, G. A.; Montgomery, J. A.; Raghavachari, K.; Al-Laham, M. A.; Zakrzewski, V. G.; Ortiz, J. V.; Foresman, J. V.; Ciolowski, J.; Stephanov, B. B.; Nanayakkara, A.; Challacombe, M.; Peng, C. Y.; Ayala, T. Y.; Chen, W.; Wong, M. W.; Andres, J. L.; Replogle, E. S.; Gomperts, R.; Martin, R. L.; Fox, V. J.; Binkley, J. S.; Defrees, D. J.; Baker, J.; Stewart, J. P.; Head-Gordon, M.; Gonzalez, C.; Pople, J. A. *Gaussian*; Gaussian Inc.: Pittsburgh, PA, 1995.

(25) Baekelandt, B. G.; Cedillo, A.; Parr, R. G. *J. Chem. Phys.* **1995**, *103*, 8548.

(26) Fuentealba, P. *J. Chem. Phys.* **1995**, *103*, 6571.

(27) Pearson, R. G. *J. Am. Chem. Soc.* **1986**, *108*, 6109.

(28) Contreras, R.; Pérez, P.; Aizman, A. *Int. J. Quantum Chem.* **1995**, *56*, 433.